# We are IntechOpen, the world's leading publisher of Open Access books Built by scientists, for scientists

6,900
Open access books available

185,000
International authors and editors

200M
Downloads

Our authors are among the

154
Countries delivered to

TOP 1%
most cited scientists

12.2%
Contributors from top 500 universities




WEB OF SCIENCE™

Selection of our books indexed in the Book Citation Index in Web of Science™ Core Collection (BKCI)

## Interested in publishing with us?
## Contact book.department@intechopen.com

Numbers displayed above are based on latest data collected.
For more information visit www.intechopen.com



Chapter 13

# A Comparison of Physical vs. Nonphysical Wedge Modalities in Radiotherapy

Hiroaki Akasaka, Naritoshi Mukumoto, Masao Nakayama, Tianyuan Wang, Ryuichi Yada, Yasuyuki Shimizu, Saki Osuga, Yuki Wakahara and Ryohei Sasaki

Additional information is available at the end of the chapter

http://dx.doi.org/10.5772/67057

**Abstract**

This chapter discusses the clinical application and implementation of wedge techniques in radiation therapy. Coverage of the target region with a curative dose is critical for treating several cancer types; to that end, wedge filters are commonly used to improve dose uniformity to the target volume. Initially, wedges designed for this purpose were physical and were made of high-density materials such as lead or steel. Subsequently, nonphysical wedges were introduced; these improved the dose uniformity using computer systems in lieu of physical materials. As wedge systems evolve, however, they each continue to have their advantages and disadvantages. When using physical wedges, it is difficult to control the generation of secondary radiation resulting from the collision of the radiation beam with the wedge body; conversely, nonphysical wedges do not create any secondary radiation because there is no physical interference with the beam. On the other hand, nonphysical wedges are less suitable for treating moving tumors, such as those in the lung, and physical wedges have better dose coverage to the target volume than nonphysical wedges. This chapter aims to guide decision-making regarding the choice of wedge types in various clinical situations.

**Keywords:** physical wedge, nonphysical wedge, radiotherapy

## 1. Introduction

Wedged techniques are routinely used in external beam radiotherapy delivery to improve the dose distribution. In earlier years, physical wedges were typically constructed from high-density materials and fixed to certain wedge angles; they were standard accessories shipped

INTECH
open science | open minds

© 2017 The Author(s). Licensee InTech. This chapter is distributed under the terms of the Creative Commons Attribution License (http://creativecommons.org/licenses/by/3.0), which permits unrestricted use, distribution, and reproduction in any medium, provided the original work is properly cited. CC BY

with linear accelerators. Such wedges are usually mounted externally or internally in the gantry head of the linear accelerators. Nonphysical wedges, first proposed in the late 1970s by Kijewski et al., produce modulated dose distributions that were similar to those of physical wedges [1]. They rely on the dynamic movements of a pair of independent collimating jaws during treatment and have been widely implemented in modern radiotherapy machines. Both modalities possess unique advantages and limitations in terms of dosimetric characteristics, treatment accuracy, and efficiency.

In this chapter, we discuss and compare the clinical implementation and application of wedge techniques in radiation therapy.

## 2. Characteristics of physical or nonphysical wedges in clinical implementation

### 2.1. Fundamental properties of physical and nonphysical wedges

In radiation therapy, wedge filters are commonly used to improve dose uniformity toward the target volume [2]. A physical wedge is usually constructed from a high-density material, such as lead or steel, which attenuates the beam progressively across the entire field. A nonphysical wedge generates a sloping dose distribution by moving one of the jaws with variable speed, while the opposite jaw remains steady. Nonphysical wedges inherently have no beam attenuation or beam hardening effect and thus offer more flexibility than physical wedges [3, 4]. According to the International Commission on Radiation Units and Measurements, the wedge angle is defined as the angle at which an isodose curve is tilted at the central axis of the beam at a specified depth (usually 10 cm) [5].

Before deciding on physical or nonphysical wedges during clinical treatment planning, the treatment planning system (TPS) requires obtaining a number of measurements from each wedge system. In general, the TPS requires data on the percentage depth-dose (PDD), beam profiles, and wedge factors of the X-ray beams [6]. As an example, **Figure 1** shows the profile curve measurements when physical or nonphysical wedges at 30° and 60° were used (field size 10 × 10 $cm^2$).

The results show that nonphysical wedges have straighter profile curve lines than physical wedges, which are desirable in clinical practice. These results are consistent with those previously described [7, 8]. Ahmad et al. reported that differences in profiles between physical and nonphysical wedges were most evident in larger fields, shallow depths, thicker wedges, and when using a low-energy beam [8].

On the other hand, the presence of a wedge filter in the path of a radiation beam decreases its intensity; this must be taken into account when calculating treatment doses. When physical wedges were used, photon energy fluence is reduced in the wedged beam compared to the open beam; this effect is more pronounced when increasing the wedge angle [9]. It has also been shown that a physical wedge factor has a stronger depth dependence than a nonphysical wedge factor owing to beam hardening [2].

http://dx.doi.org/10.5772/67057

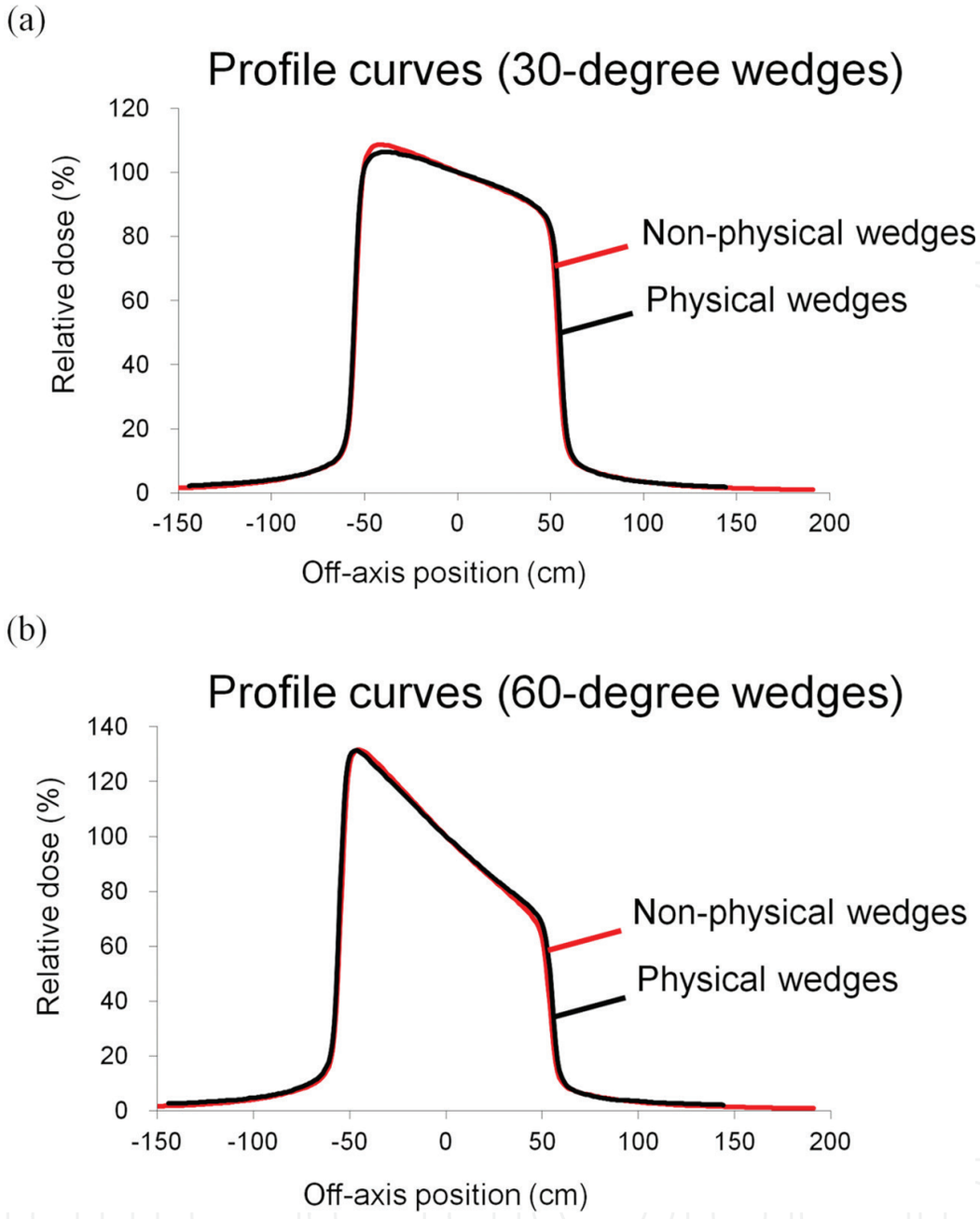



**Figure 1.** The profile curves of 10 MV X-ray beams using (a) 30° or (b) 60° of physical or nonphysical wedges under a source-surface distance of 100 cm and depth of 10 cm in water. The red line indicates profile curves of nonphysical wedges; the black line indicates that of physical wedges.

### 2.2. Comparison between calculation data and measurement data

Before wedge filters are installed in clinical practice, several measurements must be incorporated into the TPS for beam modeling. The modeling method for the TPS varies between manufacturers and also between calculation algorithms, as the mechanism of motion of the nonphysical wedges is different for every manufacturer. In this section, the Eclipse planning system (Varian Medical Systems, Palo Alto, CA, USA) and the Enhanced Dynamic Wedge (EDW, Varian Medical Systems, Palo Alto, CA, USA) are mainly described.

A physical wedge changes the beam energy fluence of the primary X-ray beam through the insertion of a metallic filter at the gantry head. This effect is modeled via a wedge transmission curve; specifically, depth doses, wedge profiles, and longitudinal profiles are used for such modeling. In the Eclipse system, the energy fluence of the primary X-ray beam is modeled as a two-dimensional spectrum that considers the mass-energy attenuation coefficient, which is calculated based on the wedge filter material and thickness. Furthermore, the physical wedge produces secondary radiation when interacting with the primary X-ray beam. Eclipse hence considers the wedge a source of scatter, and modeling is performed using a dual Gaussian plane. Moreover, when physical wedges are used in the Eclipse system, a separate electron contamination source model is applied to the calculation; it is necessary to verify the precision of the final model by comparing it to the acquired data before the wedge filters are installed in clinical practice.

Fogliata et al. compared the calculation models and measurement data using the analytical anisotropic algorithm (AAA) [10–13] and the Acuros XB (AXB) [14–16], which is built into Eclipse (version 10.0) [17]. Six and 15 MV X-rays were validated in their study; measurements were performed in water using the PTW-MP3 phantom with a 0.125 $cm^2$ cylindrical ionization chamber (Semiflex, PTW). Next, depth-dose curves were investigated for several field sizes. In the wedged field along the central axis, the difference in absolute dose between calculated vs. measured values revealed deviations (including standard deviations) smaller than 1%. Moreover, the profile curves were investigated in some field sizes at depths of $d_{max}$, 5, 10, 20, and 30 cm. In the central beam region, the average difference in profile curves between calculations and measurements was smaller than 1%, with a standard deviation lower than 1%. Output factor and monitor unit (MU) calculations were also investigated in some field sizes at a source-surface distance (SSD) of 90 cm and a depth of 5 cm in water. The difference between the calculated and measured MUs to deliver a fixed dose to the isocenter exhibited a maximum deviation of 0.2%. Therefore, when using AAA or AXB under reference conditions, it is possible to model correctly. However, when considering clinical use, validation in non-reference conditions is also necessary. Van Esch et al. validated depth-dose curves at SSDs of 80, 90, and 100 cm to verify the accuracy of modeling of the electron contamination as a function of source-to-skin distance [18]. For depth-dose curves involving different SSDs, they reported that the disagreement between calculated and measured data in the buildup region was high under conditions of higher energy and small SSD. In wedge profiles for 60° physical wedges using 18 MV for the selection of asymmetric fields (X = 15 cm, Y1 = 7.5 cm, Y2 = −5 cm), deviations up to 4% in the absolute dose at the center of the field were observed. Hence, accurate modeling using this method is difficult because the wedge produces numerous scattered photons and electrons. For tolerance settings at the time of modeling, please refer to Refs. [19, 20].

The nonphysical wedge produces a distribution similar to that of a physical wedge by moving the collimator jaw and/or modifying the dose rate. In the Varian EDW, only a single jaw is moved; moreover, the dose rate for the Siemens virtual wedge is varied. The EDW uses the segmented treatment table (STT) when planning the position of the moving jaw and corresponding doses. The golden STT (GSTT) is used for a wedge angle of 60°, which controls all other wedge fields (i.e., all the field sizes and the wedge angles) as well as the center axis dose

http://dx.doi.org/10.5772/67057

of the open field [21]. In other words, EDW settings do not require any input data for beam configuration other than the open beam data. The movement of the collimator in the EDW affects the primary radiation and scatter components, as well as the backscatter of the collimator. Therefore, it is necessary to verify the accuracy of the modeling by comparing calculated estimates to the measured data.

For the EDW, Fogliata et al. also compared the calculations to the measurements using the AAA and AXB [17]. Moreover, depth-dose curves were investigated in field sizes of 20 × 20 $cm^2$. In wedge fields along the central axis, the difference in absolute dose between the calculations and measurements presented deviations (including standard deviations) smaller than 1%. Furthermore, profile curves were investigated in a field size of 20 × 20 $cm^2$ at depths of $d_{max}$, 5, 10, 20, and 30 cm. In the central beam region, the average differences of profile curves between calculations and measurements were smaller than 1%; standard deviations were lower than 1%. Furthermore, output factors and MU calculations were investigated in some field sizes at SSDs of 90 cm and a depth of 5 cm in water. The difference between the calculated and measured MUs when delivering a fixed dose to the isocenter presented a maximum deviation of 0.2%. Validation in a selection of asymmetric fields (X = 15 cm, Y1 = 7.5 cm, Y2 = −5 cm) indicated deviations up to 1.5% in the absolute dose at the center of the field [18]. Furthermore, in a Monte Carlo simulation study, the surface dose of TPS produced large errors of up to 40% compared to Monte Carlo simulation in depth-dose curves [22]. This was attributed to two reasons: First, the calculation of PDDs with TPS is based on ionization chamber measurement data; the measurements of this chamber could be affected by contaminated electrons produced by the moving collimators. Second, the measured surface dose may be averaged incorrectly owing to the erroneous calculation of the ion chamber volume because of the partial volume effect. Monte Carlo simulation indicated that there are significant TPS errors at the outer regions of the field; the maximum relative error of the position difference between TPS and the actual measurements is 20%. Lateral electronic disequilibrium exists in the penumbra regions of the dose profile, especially for smaller field sizes. As mentioned in the American Association of Physicists in Medicine report, TPS cannot accurately calculate backscatter, multiple scattering, or electron disequilibrium in AAA [23]. It is necessary to take into account the calculation precision in the region indicated by the black arrows in **Figure 2**.

## 3. Advantages and limitations of the wedge technique in clinical applications

### 3.1. Wedge property uncertainty during treatment

Tumor motion (i.e., intrafractional organ motion) is an important consideration during radiotherapy [24]. Intrafractional motion can be caused by the respiratory, skeletal muscular, cardiac, and gastrointestinal systems. Respiratory motion in particular affects all tumor sites in the thorax and abdomen; the disease of most relevance in this case is lung cancer, as shown in **Figure 3**. Of note, respiratory motion is just one potential source of error in radiotherapy [25]. Chen et al. reported that lung tumor motion varies from 0 to 5 cm [26]; Shirato et al. reported

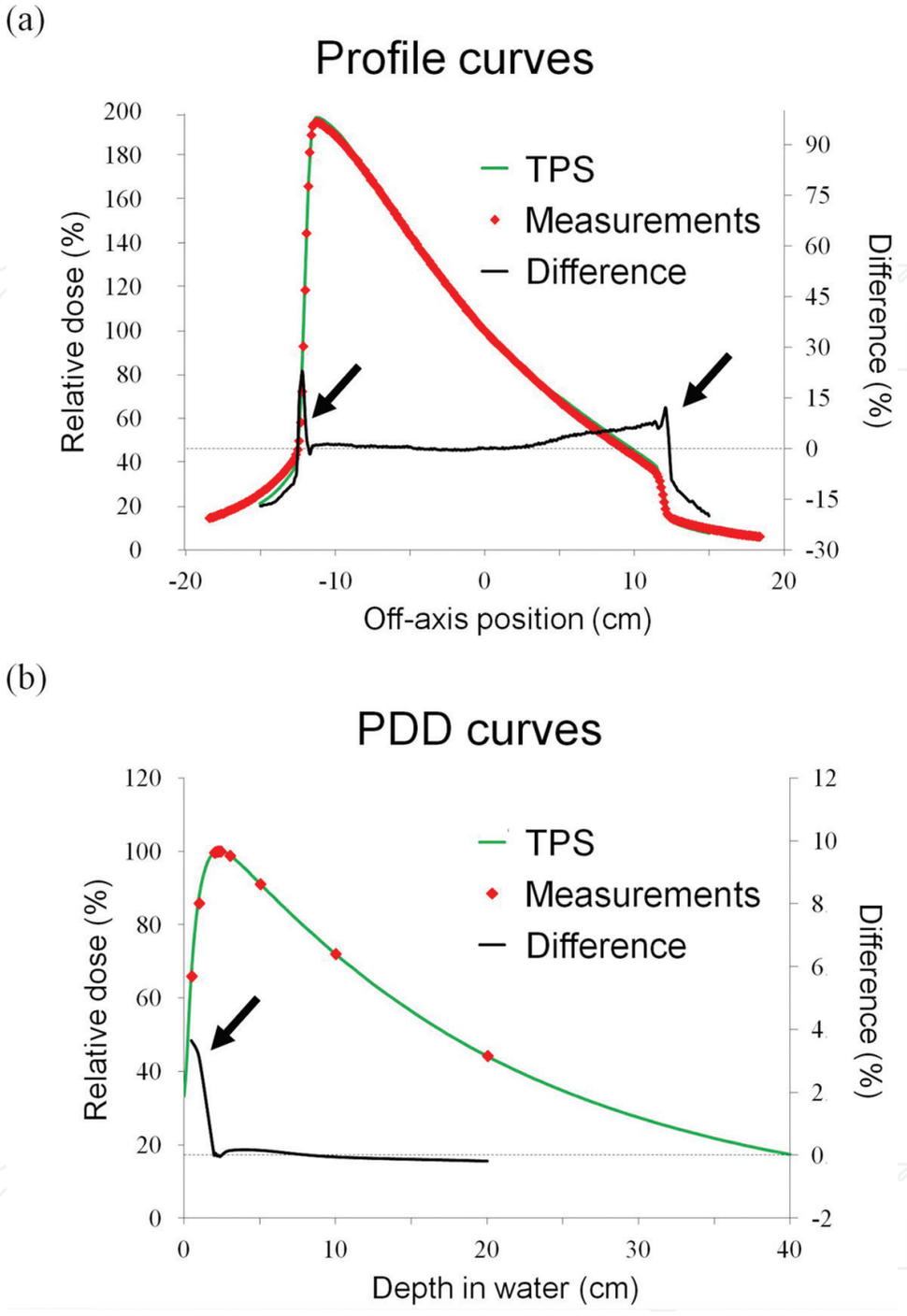



**Figure 2.** (a) Profile curves and (b) percentage depth-dose (PDD) curves of 10 MV X-ray beams in the treatment planning system (TPS) and measurements. The green line indicates TPS data, the red dots indicate measurement data, and the black line indicates the percentage of error between the TPS and actual measurements.

that the average amplitude of liver tumor motion was up to 1.9 cm [27], while Hamlet et al. reported that the larynx elevates approximately 2 cm while swallowing [28].

Intrafractional organ motion can result in two types of effect. The first is the "dose-blurring effect," which results in the over/under dosage of the tumor with radiation. The second is

http://dx.doi.org/10.5772/67057

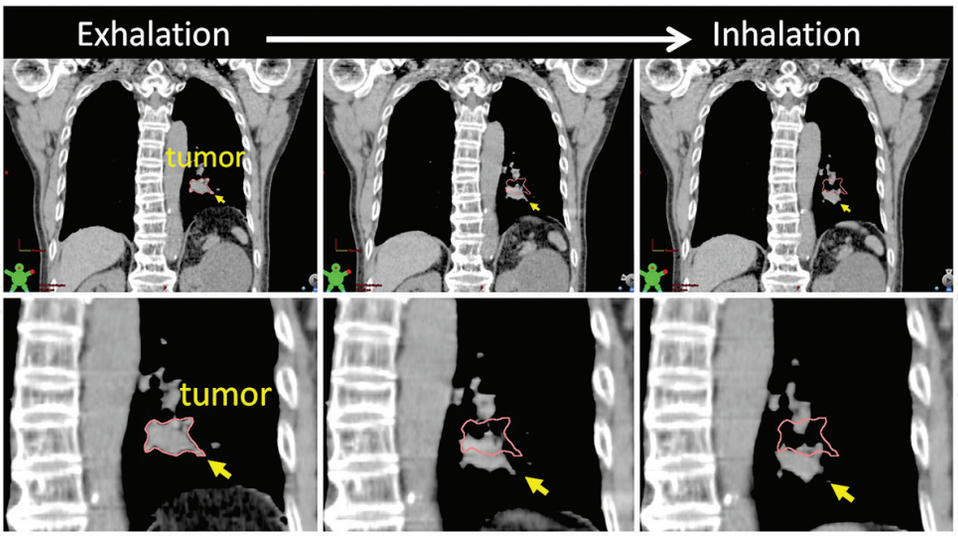



**Figure 3.** The change over time of tumor motion in the lung between exhalation and inhalation. The red line indicates the contour of the tumor during exhalation; the tumor moves up and down markedly during breathing.

termed the "interplay effect," which is only a problem in the case of dynamic delivery of intensity-modulated radiation therapy or dynamic treatments with nonphysical wedges. This effect is the result of interplay between the moving tumor and the motion of the radiation beam as defined by the nonphysical wedges [29, 30] and can result in dose discrepancy.

The respiratory-based interplay effects for nonphysical wedges have previously been studied; it was reported that approximately 50% of the organ receives a dose 5–15% higher than that prescribed when the collimator is moved from the caudal to the cranial direction. Conversely, collimator movement in the opposite direction results in under-dosing [29]. Moreover, Kakakhel et al. estimated the interplay effects for nonphysical wedges in a phantom study and reported that more than 90% of the area of the target region was covered by the prescribed dose when the phantom was rested. However, for a moving phantom, less than 70% of the target region was covered by the prescribed dose [24].

For the reasons stated above, nonphysical wedges should be considered with caution before utilization for treatment in cases of respiratory organ motion. On the other hand, physical wedges have limited field sizes, densities, and composition materials; hence, they create more low-energy electrons and photon-scattering radiation than nonphysical wedges [31]. Furthermore, the dose outside the field using nonphysical wedges is half that of physical wedges [32].

### 3.2. Appropriate choice whether physical or nonphysical wedge at several irradiation situations

The choice of physical vs. nonphysical wedges is critical in several clinical situations. As mentioned above, nonphysical wedges have more liabilities than physical wedges for the treatment of moving tumors. In contrast, physical wedges create more secondary radiation than nonphysical wedges. Petrovic et al. reported that the peripheral dose of the nonphysical wedge field is half that of the physical wedge field; this is owing to scatter outside the physi-

cal wedge field that arises from the interaction of the beam with the material of the physical wedge (such interactions include Compton scattering).

Clinically, this provides an advantage to the nonphysical wedge field [32]. The effect of secondary radiation outside the field is an important consideration for breast cancer treatment. For example, **Figure 4** shows how the low-dose area was expanded to the opposite breast when using physical wedges; such secondary radiation exposure may precipitate the development of another tumor. Warlic et al. reported that the average dose outside of the field with a nonphysical wedge was 2.7–2.8%, whereas the dose was 4.0–4.7% with a physical wedge. The nonphysical wedge is hence a practical advance that improves the dose distribution in patients undergoing breast conservation while simultaneously minimizing the dose to the contralateral breast, thereby reducing potential carcinogenic effects [33].

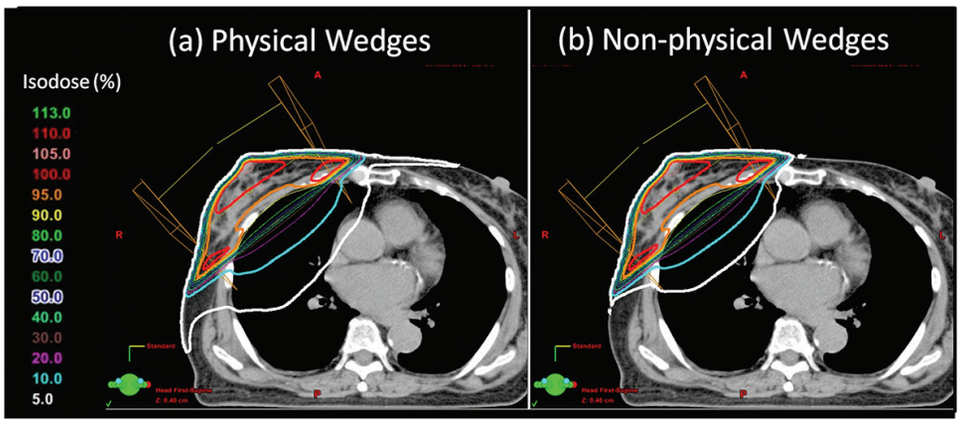



**Figure 4.** The dose distributions of radiotherapy in a breast cancer patient using (a) physical wedges or (b) nonphysical wedges. Each line indicates the dose corresponding to each treatment intensity planning.

Nonphysical wedges have significant benefits for both the therapists and patients. Saminathan et al. reported that the number of MUs used to deliver a particular dose using a nonphysical wedge field is less than that used for a physical wedge field [2]. Moreover, Njeh reported that using nonphysical wedges results in significant dose reductions to areas outside of the treatment field [34]. The reduction of MUs can also result in minimizing treatment times; this benefits patients who have worse performance statuses.

## 4. Conclusions

Each of the two wedge types, physical and nonphysical, has several characteristics that produce both advantages and disadvantages under specific conditions. Clinicians should choose between physical and nonphysical wedges with careful consideration to tumor motion, the effect of secondary radiation, and the performance status of the patient.

## Author details

Hiroaki Akasaka*, Naritoshi Mukumoto, Masao Nakayama, Tianyuan Wang, Ryuichi Yada, Yasuyuki Shimizu, Saki Osuga, Yuki Wakahara and Ryohei Sasaki

*Address all correspondence to: akasaka@harbor.kobe-u.ac.jp

Division of Radiation Oncology, Kobe University Graduate School of Medicine, Kobe City, Hyogo, Japan

## References

[1] Kijewski PK, Chin LM, Bjärngard BE. Wedge-shaped dose distributions by computer-controlled collimator motion. Med Phys. 1978;**5**:426–429.

[2] Saminathan S, Manickam R, Supe SS. Comparison of dosimetric characteristics of physical and enhanced dynamic wedges. Rep Pract Oncol Radiother. 2001;**17**:4–12. DOI: 10.1016/j.rpor.2011.06.007.

[3] Klein EE, Low DA, Meigooni AS, Purdy JA. Dosimetry and clinical implementation of dynamic wedge. Int J Radiat Oncol Biol Phys. 1995;**31**:583–592.

[4] Shih R, Lj XA, Hsu WL. Dosimetric characteristics of dynamic wedged fields: a Monte Carlo study. Phys Med Biol. 2001;**46**:N281–N292.

[5] Cherry P, Duxbury A, editors. Practical radiotherapy physics and equipment. New York, NY: Oxford University Press; 1998. 252 p.

[6] Caprile PF, Venencia CD, Besa P. Comparison between measured and calculated dynamic wedge dose distributions using the anisotropic analytic algorithm and pencil-beam convolution. J Appl Clin Med Phys. 2006;**8**;47–54.

[7] Avadhani JS, Pradhan AS, Sankar A, Viswanathan PS. Dosimetric aspects of physical and of Clinac 2100c linear accelerator. Strahlenther Onkol. 1997;**173**:524–528.

[8] Ahmad M, Hussain A, Muhammad W, Rizvi SQ, Matiullah. Studying wedge factors and beam profiles for physical and enhanced dynamic wedges. J Med Phys. 2010;**35**:33–41. DOI: 10.4103/0971-6203.57116.

[9] Geraily G, Mirzapour M, Mahdavi SR, Allahverdi M, Mostaar A, Masoudifar M. Monte Carlo study on beam hardening effect of physical wedges. Int J Radial Res. 2014;**12**:249–256. DOI: 10.1016/S0939-3889(15)70758-0.

[10] Ulmer W, Harder D. A triple Gaussian pencil beam model for photon beam treatment planning. Z Med Phys. 1995;**5**:25–30. DOI: 10.1016/S0939-3889(15)70758-0.

[11] Ulmer W, Harder D. Applications of a triple Gaussian pencil beam model for photon beam treatment planning. Z Med Phys. 1996;**6**:68–74. DOI: 10.1016/S0939-3889(15)70784-1.

[12] Ulmer W, Pyyry J, Waissl W. A 3D photon superposition/convolution algorithm and its foundation on results of Monte Carlo calculations. Phys Med Biol. 2005;**50**:1767–1790. DOI: 10.1088/0031-9155/50/8/010.

[13] Sievinen J, Ulmer W, Kaissl W. AAA photon dose calculation model in Eclipse™. Palo Alto (CA): Varian Medical Systems. 2005;**118**:2894.

[14] Vassiliev ON, Wareing TA, McGhee J, Failla G, Salehpour MR, Mourtada F. Validation of a new grid-based Boltzmann equation solver for dose calculation in radiotherapy with photon beams. Phys Med Biol. 2010;**55**:581–598. DOI: 10.1088/0031-9155/55/3/002.

[15] Fogliata A, Nicolini G, Clivio A, Vanetti E, Cozzi L. Dosimetric evaluation of Acuros XB advanced dose calculation algorithm in heterogeneous media. Radiat Oncol. 2011;**6**:82. DOI: 10.1186/1748-717X-6-82.

[16] Bush K, Gagne IM, Zavgorodni S, Ansbacher W, Beckham W. Dosimetric validation of Acuros XB with Monte Carlo methods for photon dose calculations. Med Phys. 2011;**38**:2208–2221. DOI: 10.1118/1.3567146

[17] Fogliata A, Nicolini G, Clivio A, Vanetti E, Mancosu P, Cozzi L. Dosimetric validation of the Acuros XB Advanced Dose Calculation algorithm: fundamental characterization in water. Phys Med Biol. 2011;**56**:1879–1904. DOI: 10.1088/0031-9155/56/6/022.

[18] Van Esch A, Tillikainen L, Pyykkonen J, Tenhunen M, Helminen H, Siljamäki S, Alakuijala J, Paiusco M, Lori M, Huyskens DP. Testing of the analytical anisotropic algorithm for photon dose calculation. Med Phys. 2006;**33**:4130–4148. DOI: 10.1118/1.2358333

[19] Fraass B, Doppke K, Hunt M, Kutcher G, Starkschall G, Stern R, Van Dyke J. American Association of Physicists in Medicine Radiation Therapy Committee Task Group 53: quality assurance of clinical radiotherapy treatment planning. Med Phys. 1998;**25**:1773–1829. DOI: 10.1118/1.598373.

[20] Mijnheer B, Olszewska A, Fiorino C, Hartmann G, Knöös T, Rosenwald JC, Welleweerd H. Quality assurance of treatment planning systems practical examples for non-IMRT photon beams (Vol. 1). Brussels: ESTRO; 2004. 96 p.

[21] Rodrigues C, Batel V, Germano S, Grillo IM, Pinto JL. Dosimetric study of enhanced dynamic wedges to clinical implementation into XiO treatment planning system. Electrónica e Telecomunicações. 2007;**4**:838–841.

[22] Chang KP, Chen LY, Chien YH. Monte Carlo simulation of linac irradiation with dynamic wedges. Radiat Prot Dosimetry. 2014;**162**:24–28. DOI: 10.1093/rpd/ncu211.

[23] American Association of Physicists in Medicine. Tissue inhomogeneity corrections for megavoltage photon beams: Report of Task Group No. 65. Madison, WI: Medical Physics Publishing; 2004. 135 p.

[24] Kakakhel MB, Kairn T, Kenny J, Seet K, Fielding AL, Trapp JV. Interplay effects during enhanced dynamic wedge deliveries. Phys Med. 2013;**29**:323–332. DOI: 10.1016/j.ejmp.2012.04.007.

[25] Keall PJ, Mageras GS, Balter JM, Emery RS, Forster KM, Jiang SB, Kapatoes JM, Low DA, Murphy MJ, Murray BR, Ramsey CR, Van Herk MB, Vedam SS, Wong JW, Yorke E. The management of respiratory motion in radiation oncology report of AAPM Task Group 76. Med Phys. 2006;**33**:3874–3900. DOI: 10.1118/1.2349696.

[26] Chen QS, Weinhous MS, Deibel FC, Ciezki JP, Macklis RM. Fluoroscopic study of tumor motion due to breathing: facilitating precise radiation therapy for lung cancer patients. Med Phys. 2001;**28**:1850–1856. DOI: 10.1118/1.1398037.

[27] Shirato H, Seppenwoolde Y, Kitamura K, Onimura R, Shimizu S. Intrafractional tumor motion: lung and liver. Semin Radiat Oncol. 2004;**14**:10–18. DOI: 10.1053/j.semradonc.2003.10.008

[28] Hamlet S, Ezzell G, Aref A. Larynx motion associated with swallowing during radiation therapy. Int J Radiat Oncol Biol Phys. 1994;**28**:467–470. DOI: 10.1016/0360-3016(94)90073-6.

[29] Pemler P, Besserer J, Lombriser N, Pescia R, Schneider U. Influence of respiration-induced organ motion on dose distributions in treatments using enhanced dynamic wedges. Med Phys. 2001;**28**:2234–2240. DOI: 10.1118/1.1410121.

[30] Isa M, Iqbal K, Afzal M, Buzdar S, Chow J. Physical and dynamic wedges in radiotherapy for rectal cancer: a dosimetric comparison. Med Phys. 2012;**39**:4636.

[31] Klein EE, Esthappan J, Li Z. Surface and buildup dose characteristics for 6, 10, and 18 MV photons from an Elekta Precise linear accelerator. J Appl Clin Med Phys. 2003;**4**:1–7. DOI: 10.1120/1.1520113.

[32] Petrovic B, Grzadziel A, Rutonjski L, Slosarek K. Linear array measurements of enhanced dynamic wedge and treatment planning system (TPS) calculation for 15 MV photon beam and comparison with electronic portal imaging device (EPID) measurements. Radiol Oncol. 2010;**44**:199–206. DOI: 10.2478/v10019-010-0037-5.

[33] Warlick WB, O'Rear JH, Earley L, Moeller JH, Gaffney DK, Leavitt DD. Dose to the contralateral breast: a comparison of two techniques using the enhanced dynamic wedge versus a standard wedge. Med Dosim. 1997;**22**:185–191.

[34] Njeh CF. Enhanced dynamic wedge output factors for Varian 2300CD and the case for a reference database. J Appl Clin Med Phys. 2015;**16**:5498.

IntechOpen

IntechOpen